Oscillator Strengths of Quantum Transitions in Spherical Quantum Dot GaAs/$Al_xGa_{1-x}As$/GaAs/$Al_xGa_{1-x}As$ with On-Center Donor Impurity

V. Holovatsky*, I. Bernik and O. Voitsekhivska
Chernivtsi National University, Kotsubynsky str., 2, Chernivtsi, 58012, Ukraine

(Received April 15, 2013; in final form September 26, 2013)

The investigation of the electron and hole energies and probability densities is performed for the cases with and without the donor hydrogenic impurity placed into the centre of quantum dot quantum well structures with different thicknesses of layers. The oscillator strengths of intra- and interband quantum transitions in GaAs/$Al_xGa_{1-x}As$ core/shell/well/shell spherical quantum dot with ionized on-center donor impurity are estimated. The oscillator strengths of quantum transitions non-monotonously depend on the width of the layers due to the different location of carriers. The optimal geometrical parameters of the nanostructure are estimated for the possibility of multicolor light emission based on interband quantum transitions.

DOI: 10.12693/APhysPolA.125.93
PACS 73.21.La, 78.67.Hc, 71.55.−i

1. Introduction

The semiconductor low-dimensional quantum heterostructures (i.e. quantum wells, wires, and dots) are conspicuous in many technological applications such as infrared photodetectors [1], lasers [2, 3], light emitting diodes [4–6], single electron transistors [7], etc. The modern advances in semiconductor technology allow the preparation of more complex structures than the simple quantum wells, wires, or dots. Such structures as multiple quantum rings [8], complex quantum wires [9, 10] and the quantum dot quantum well (QDQW) structures [11–15] are extensively studied. QDQW structures are the multilayered quantum dots, composed of two semiconductor materials: the one with the larger bulk band gap is sandwiched between a core and an outer shell of the material with smaller bulk band gap and embedded into the matrix. QDQW structures are applied for the fabrication of white light emission sources. Recently, QDQW structures that achieved multicolor emission were investigated.

The spectra of quasi-particles in QDQWs and influence of geometric parameters and doped impurities is to be studied in detail in order to assure that the white light sources can be produced on their base. The pioneer theoretical and experimental investigations of multilayered spherical nanostructures were performed in [16, 17]. The results of calculations of interband transitions energies obtained within the effective mass approximation correlated well with the experimental data even when the size of the certain layer of nanostructure was 1–2 lattice constants. Besides, in the framework of this method, the energy spectra of the electrons in AlGaAs/GaAs quantum rings with the sizes of 2–4 nm [18, 19] were studied and the results of numeric calculations and experimental data correlated, too. Thus, the effective mass approximation remains the basic theoretical method because using it one can obtain the exact solutions of the Schrödinger equations even for the multilayered systems.

The analysis of the energies and probability densities of carriers in QDQWs was performed in [11–15]. It was shown that the energies and localization of carriers in these structures depend, mainly, on the core radius and shells sizes. It is well known that an impurity realizes the important effect at the optical properties of QDQWs, too. The presence of charged impurity in QD changes the potential of size quantization, affecting both the quasiparticles energy spectra and oscillator strengths of radiation transitions. The hydrogenic impurity states in QDs were widely studied by many authors [20–25]. The general theories of quasiparticles energy spectra in spherical nanosystems with shallow impurities in QD: quantum antidot with donor impurity [20] and QD with acceptor impurity [21] were developed. In [22], the energy spectrum and wave functions of electron in multi-shell QD with donor impurity were obtained in the framework of the effective mass approximation using the variational method.

In [23–25] the electronic and optical properties of QDQWs with donor impurities were investigated. In [23], the oscillator strengths of electron intraband quantum transitions in spherical QDQW with or without donor impurity were obtained within rectangular potential barriers and effective mass approximation using the shooting method for the numerical solving of the Schrödinger equation. In [24], the oscillator strengths of intraband quantum transitions for the electron in GaAs/$Al_xGa_{1-x}As$ multishell spherical QD with parabolic confinement and on-center donor impurity were calculated. In [25] the exact and variational calculations of a hydrogenic impurity binding energy in QDQW were performed taking into account different effective masses and dielectric constants of nanosystem layers.

*corresponding author; e-mail: ktf@chnu.edu.ua

These theoretical investigations prove that when the on-center impurity is present in nanostructure, the maximal shift of energy levels is observed and the intensities of interband transitions are not changed essentially. For the case of non-center impurity the intensities of transitions sharply reduce due to the different location of electron and hole. It is clear that the on-center impurity can serve as an additional mechanism guiding the energies of quantum transitions.

In this paper we study the optical properties of GaAs/$Al_xGa_{1-x}As$ multishell spherical QD with step-like confinement potential with and without a hydrogenic on-center donor impurity. In this context, we obtain the exact energy spectrum and wave functions of electron and hole in the field of on-center donor impurity in the framework of the effective mass approximation. The oscillator strengths of $1p$–$1s$ and $2p$–$1s$ intraband transitions together with $1s$–$1s$ and $1p$–$1p$ interband transitions are calculated for QDQW with different sizes of core and shells. The results are compared for the cases with and without the donor impurity.

2. Spectra and wave functions of electron and hole in QDQW $GaAs/Al_xGa_{1-x}As/GaAs/Al_xGa_{1-x}As$ with donor impurity

We consider the multilayered spherical QD composed of a core GaAs ("0") and two spherical shells $Al_xGa_{1-x}As$ and GaAs ("1", "2") embedded into a semiconductor matrix ("3"). The radius of the core-well is r_0, the barrier width is Δ and the outer shell-well width is ρ. The impurity is placed into the center of the QD. The potential energies of electron and hole are shown in Fig. 1a and b, respectively.

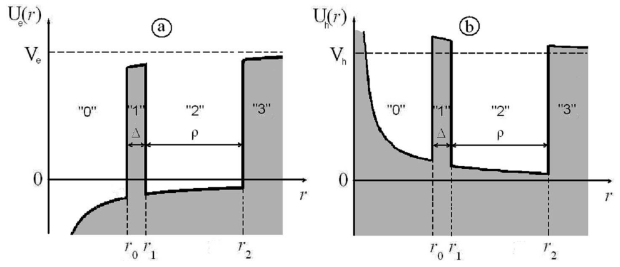

Fig. 1. Potential energy of electron (a) and hole (b) in QDQW $GaAs/Al_xGa_{1-x}As/GaAs/Al_xGa_{1-x}As$ with on-center donor impurity.

The Schrödinger equation for the electron and hole is written as

$$-\frac{\hbar^2}{2}\boldsymbol{\nabla}\frac{1}{\mu_{\rm e,h}(r)}\boldsymbol{\nabla}\Psi^{\rm e,h}_{nlm}(\boldsymbol{r})+\Big[U_{\rm e,h}(r)\pm U_{\rm imp}(r)+U^p_{\rm e,h}(r)\Big]\Psi^{\rm e,h}_{nlm}(\boldsymbol{r})=E^{\rm e,h}_{nl}\Psi^{\rm e,h}_{nlm}(\boldsymbol{r}). \quad (1)$$

The sign "+" is taken for the electron and "–" is for the hole. The effective masses and confining potentials are given by the formulae

$$\mu_{\rm e,h}(r)=\begin{cases} m^{\rm e,h}_0, & r\le r_0, \quad r_1<r\le r_2,\\ m^{\rm e,h}_1, & r_0<r\le r_1, \quad r>r_2,\end{cases} \quad (2)$$

$$U_{\rm e,h}(r)=\begin{cases} 0, & r\le r_0, \quad r_1<r\le r_2,\\ V_{\rm e,h}, & r_0<r\le r_1, \quad r>r_2.\end{cases} \quad (3)$$

The potential energy of electron in the field of on-center impurity, taking into account the mismatch of dielectric constants of different media, $U_{\rm imp}(r)$ is written as

$$U_{\rm imp}(r)=\begin{cases} -\frac{e^2}{\varepsilon_0 r}+\frac{e^2}{\varepsilon_0 r_0}\left(1-\frac{\varepsilon_0}{\varepsilon_1}\right)+\frac{e^2}{\varepsilon_1 r_1}\left(1-\frac{\varepsilon_1}{\varepsilon_0}\right)+\frac{e^2}{\varepsilon_0 r_2}\left(1-\frac{\varepsilon_0}{\varepsilon_1}\right), & r<r_0,\\ -\frac{e^2}{\varepsilon_1 r}+\frac{e^2}{\varepsilon_1 r_1}\left(1-\frac{\varepsilon_1}{\varepsilon_0}\right)+\frac{e^2}{\varepsilon_0 r_2}\left(1-\frac{\varepsilon_0}{\varepsilon_1}\right), & r_0\le r<r_1,\\ -\frac{e^2}{\varepsilon_0 r}+\frac{e^2}{\varepsilon_0 r_2}\left(1-\frac{\varepsilon_0}{\varepsilon_1}\right), & r_1\le r<r_2,\\ -\frac{e^2}{\varepsilon_1 r}, & r\ge r_2,\end{cases} \quad (4)$$

where ε_0 and ε_1 are the dielectric constants of GaAs and $Al_xGa_{1-x}As$, respectively. $U^p_{\rm e,h}(r)$ — the potential energy of electron and hole taking into account their interaction with polarization charges induced on structure interfaces.

Considering the small difference between the dielectric constants, the potential energy (4) can be replaced by the approximated expression $U_{\rm imp}(r)\approx -e^2/(\varepsilon r)$ with averaged dielectric constant $\varepsilon=(\varepsilon_0+\varepsilon_1)/2$. Herein, the largest error (at $r=0$ and $r>r_2$) does not exceed 4% and in the region where the quasiparticle is mainly located, its value is less than 2%. The contribution of the term $U^p_{\rm e,h}(r)$ can be ignored comparing to the confining potential and the Coulomb potential of interaction between quasiparticles and impurity due to the small value of the coefficient $(\varepsilon_0-\varepsilon_1)/(\varepsilon_0+\varepsilon_1)$.

Considering the spherical symmetry of the structure, we obtain the equations for the radial parts of electron and hole wave functions

$$-\frac{\hbar^2}{2m^{\rm e,h}_0}\left[\frac{\partial^2}{\partial r^2}+\frac{2}{r}\frac{\partial}{\partial r}-\frac{\ell(\ell+1)}{r^2}\right]R^{\rm e,h}_{n\ell}(r)\mp\frac{e^2}{\varepsilon r}R^{\rm e,h}_{n\ell}(r)=E^{\rm e,h}_{n\ell}R^{\rm e,h}_{n\ell}(r), \quad r\le r_0, \quad r_1<r\le r_2, \quad (5)$$

$$-\frac{\hbar^2}{2m^{\rm e,h}_1}\left[\frac{\partial^2}{\partial r^2}+\frac{2}{r}\frac{\partial}{\partial r}-\frac{\ell(\ell+1)}{r^2}\right]R^{\rm e,h}_{n\ell}(r)+\left(V_{\rm e,h}\mp\frac{e^2}{\varepsilon r}\right)R^{\rm e,h}_{n\ell}(r)=E^{\rm e,h}_{n\ell}R^{\rm e,h}_{n\ell}(r),$$

$$r_0<r\le r_1, \quad r>r_2. \quad (6)$$

The general solutions of Eqs. (5), (6) have the form

$$R^{\mathrm{e,h}}_{n\ell}(r) = \begin{cases} \exp\left(-\xi^{\mathrm{e,h}}_0 r/2\right) r^{\ell}\left[A^{\mathrm{e,h}}_i F(\ell+1-\eta^{\mathrm{e,h}}_0, 2\ell+2, \xi^{\mathrm{e,h}}_0 r) \right. \\ \left. \quad + B^{\mathrm{e,h}}_i G(\ell+1-\eta^{\mathrm{e,h}}_0, 2\ell+2, \xi^{\mathrm{e,h}}_0 r)\right], \\ \quad r \le r_0, \quad r_1 < r \le r_2, \\ \exp\left(-\xi^{\mathrm{e,h}}_1 r/2\right) r^{\ell}\left[A^{\mathrm{e,h}}_{i+1} F(\ell+1-\eta^{\mathrm{e,h}}_1, 2\ell+2, \xi^{\mathrm{e,h}}_1 r) \right. \\ \left. \quad + B^{\mathrm{e,h}}_{i+1} G(\ell+1-\eta^{\mathrm{e,h}}_1, 2\ell+2, \xi^{\mathrm{e,h}}_1 r)\right], \\ \quad r_0 < r \le r_1, \quad r > r_2, \end{cases} \quad i = 0, 2, \quad (7)$$

where $F(a,b,z)$ and $G(a,b,z)$ are the confluent hypergeometrical functions of the first and the second type,

$$\xi^{\mathrm{e,h}}_0 = \frac{\sqrt{8m^{\mathrm{e,h}}_0(-E^{\mathrm{e,h}}_{n\ell})}}{\hbar}, \quad \eta^{\mathrm{e,h}}_0 = \pm\frac{2m^{\mathrm{e,h}}_0 e^2}{\varepsilon_0 \xi^{\mathrm{e,h}}_0 \hbar^2},$$

$$\xi^{\mathrm{e,h}}_1 = \frac{\sqrt{8m^{\mathrm{e,h}}_1(V^{\mathrm{e,h}} - E^{\mathrm{e,h}}_{n\ell})}}{\hbar}, \quad \eta^{\mathrm{e,h}}_1 = \pm\frac{2m^{\mathrm{e,h}}_1 e^2}{\varepsilon_0 \xi^{\mathrm{e,h}}_1 \hbar^2}. \quad (8)$$

The coefficients $B^{\mathrm{e,h}}_0 = 0$ and $A^{\mathrm{e,h}}_3 = 0$ because the wave functions are limited at $r = 0$ and $r \to \infty$. The other coefficients and quasiparticles energies are obtained from the condition of wave functions and their densities of currents continuity

$$\begin{cases} R^{\mathrm{e,h}}_{n\ell\ i}(r_i) = R^{\mathrm{e,h}}_{n\ell\ i+1}(r_i), \\ \frac{1}{m^{\mathrm{e,h}}_i}\frac{\partial R^{\mathrm{e,h}}_{n\ell\ i}(r)}{\partial r}\Big|_{r_i} = \frac{1}{m^{\mathrm{e,h}}_{i+1}}\frac{\partial R^{\mathrm{e,h}}_{n\ell\ i+1}(r)}{\partial r}\Big|_{r_i}, \end{cases} \quad i = 0, 1, 2, \quad (9)$$

and normality condition

$$\int_0^{\infty} \left|R^{\mathrm{e,h}}_{n\ell}(r)\right|^2 r^2 \mathrm{d}r = 1. \quad (10)$$

In dipole approximation, the oscillator strengths of interband quantum transitions are proportional to the square of wave functions overlapping integral [22]:

$$F_{\mathrm{i-f}} \sim E^{-1}\left|\int \psi^{\mathrm{e}}_{\mathrm{i}}(\boldsymbol{r}_{\mathrm{e}})\psi^{\mathrm{h}}_{\mathrm{f}}(\boldsymbol{r}_{\mathrm{h}})\delta(\boldsymbol{r}_{\mathrm{e}} - \boldsymbol{r}_{\mathrm{h}})\,\mathrm{d}\boldsymbol{r}\right|^2, \quad (11)$$

where E is the energy of quantum transition, given by formula

$$E = E^{\mathrm{e}}_{\mathrm{i}} + E^{\mathrm{h}}_{\mathrm{f}} + E_{\mathrm{g}}. \quad (12)$$

The selection rule for the interband transitions is $\Delta\ell = 0$. We are going to perform the numerical computation of oscillator strengths of interband quantum transitions between the ground states (F_{1s-1s}) and the first excited states (F_{1p-1p}) for the electron and hole.

The oscillator strengths of intraband quantum transitions in dipole approximation are written according to [23] as

$$F_{\mathrm{i-f}} \sim (E^{\mathrm{e}}_{\mathrm{i}} - E^{\mathrm{e}}_{\mathrm{f}})\left|\int \psi^{\mathrm{e}*}_i(\boldsymbol{r}) r\cos\theta \psi^{\mathrm{e}}_{\mathrm{f}}(\boldsymbol{r})\,\mathrm{d}\boldsymbol{r}\right|^2. \quad (13)$$

The selection rule for the intraband transitions is $\Delta\ell = \pm 1$. We are going to calculate the oscillator strengths of intraband transitions from $1p$- and $2p$-states to ground state.

3. Analysis of the results

The computer calculations were performed using the physical parameters of $Al_xGa_{1-x}As$ semiconductor with Al concentration $x = 0$ for the potential wells and $x = 0.4$ for the barriers: $m^{\mathrm{e}}_0 = 0.067m_{\mathrm{e}}$, $m^{\mathrm{e}}_1 = 0.1002m_{\mathrm{e}}$, $V_{\mathrm{e}} = 297.08$ meV, $m^{\mathrm{h}}_0 = 0.51m_{\mathrm{e}}$, $m^{\mathrm{h}}_1 = 0.61m_{\mathrm{e}}$, $V_{\mathrm{h}} = 224.12$ meV, $\varepsilon_0 = 12.9$, $\varepsilon_1 = 11.8$, $a_0 = 0.5653$ nm, $a_1 = 0.5656$ nm, where m_{e} — the mass of pure electron.

The electron and hole ground ($1s$) and first excited ($1p$) states energies $E^{\mathrm{e,h}}_{nl}$ (for QDQW with the impurity) as functions of well width (ρ) at fixed core radius $r_0 = 6$ nm and shell width $\Delta = 2$ nm are presented in Fig. 2. The electron and hole energies $E^{(0)\mathrm{e,h}}_{nl}$ (for QDQW without the impurity) are plotted by thin curves for the comparison. It is clear that all energy dependences on well width are non-monotonous and decaying. It is explained due to the distribution of the probability densities of quasiparticles location in nanostructure. The regions of slight change of the energies correspond to the case when the quasiparticles are located inside the core. Herein, the variation of shell-well width weakly changes the energy. When the electron or hole (in certain state) is located in outer well, the increase of its width causes the strong decrease of quasi-particles energy. Figure proves that the impurity more affects quasiparticles energies when they are located inside the core. Besides, the effect on s-states is bigger than on p-states. The electron energy decreases due to the impurity attraction and the hole one increases due to the impurity repulsion.

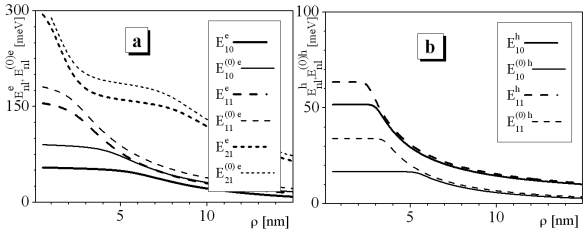

Fig. 2. Electron energy in $1s$-, $1p$- and $2p$-state (a) and hole energy in $1s$- and $1p$-state (b) as functions of outer shell-well width (ρ) at core-well radius $r_0 = 6$ nm and barrier width $\Delta = 2$ nm.

Varying the widths of QDQW layers one can obtain the demanded energy of quantum transitions. The sufficient value of oscillator strength is required to realize the quantum transition in practice. The oscillator strengths depend not only on the energies of quasiparticles but also on their location in the nanostructure in different states, formulae (11)–(14). Therefore, the urgent problem is to investigate the influence of impurity and geometrical sizes of the layers on the distribution of electron and hole radial densities.

In Figs. 3, 4 the distributions of electron and hole densities in $1s$-, $1p$-, $2p$-states at different outer well and barrier widths are shown for the cases with the impurity in nanostructure or without it. The varying geometrical

parameters and presence of impurity essentially influence on the quasiparticles location in the nanostructure.

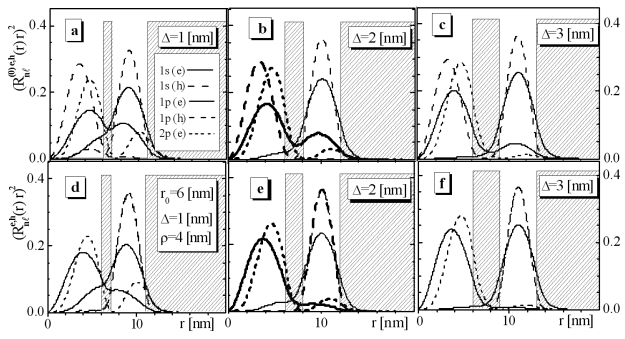

Fig. 3. Distributions of electron and hole radial probability densities for the case without the impurity (a)–(c) and with on-center impurity (d)–(f) in the nanostructure with parameters: $r_0 = 6$ nm, $\rho = 4$ nm, $\Delta = 1, 2, 3$ nm.

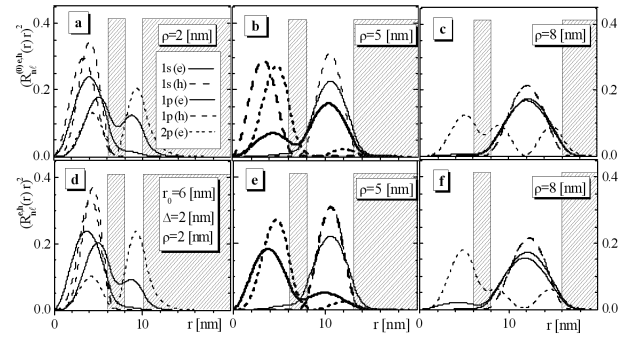

Fig. 4. Distributions of electron and hole radial probability densities for the case without the impurity (a)–(c) and with on-center impurity (d)–(f) in the nanostructure with parameters: $r_0 = 6$ nm, $\Delta = 2$ nm, $\rho = 2, 5, 8$ nm.

From Fig. 3a–c one can see that the increasing barrier width entails the enhancement of electron and hole $1s$-state wave functions overlapping when the impurity is absent. When the on-center impurity is present, the increasing Δ causes the quasiparticles spatial separation due to the electron is attracted and the hole is repulsed by donor impurity. Herein, the overlapping of wave functions is reduced, Fig. 3d–f.

The same situation is observed in Fig. 4 at the varying shell-well width (ρ). In case without the impurity, the electron primarily locates in outer shell-well when its width increases because its effective mass is smaller than the hole one. When the impurity is present, the electron tunnels into outer well at bigger ρ than the hole. From Figs. 3, 4 one can see that the electron in $1p$- and $2p$-states is located in different potential wells.

The behavior of quasiparticles displays on the dependences of oscillator strengths of quantum transitions on geometrical parameters of nanostructure shown in Fig. 5. Figure proves that the oscillator strengths both for intra- and interband transitions have complicated dependences on core-well radius (r_0), barrier width (Δ) and shell-well width (ρ). Maximal and minimal values of oscillator strengths correspond to the big and small overlapping of quasiparticles wave functions.

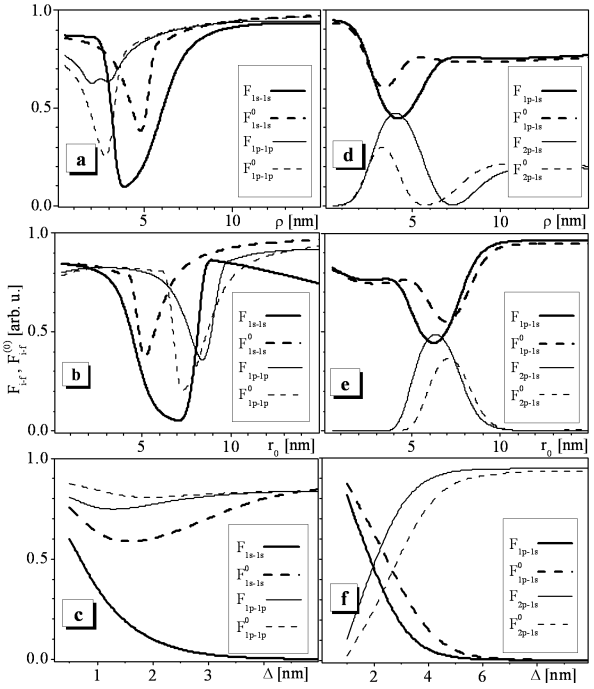

Fig. 5. Oscillator strength of interband (a)–(c) and intraband (d)–(f) transitions as functions of: well width ρ at core radius $r_0 = 6$ nm and shell width $\Delta = 2$ nm (a), (d); core radius r_0 at $\Delta = 2$ nm, $\rho = 4$ nm (b), (e); shell thickness Δ at $r_0 = 6$ nm and $\rho = 4$ nm (c), (f).

Using the presented dependences of oscillator strengths of quantum transitions one can explicate the optimal geometrical parameters of nanostructure layers in order to obtain the demanded physical characteristics. For example, in order to fabricate the light source based on two simultaneous interband transitions with the energies which can be correlated by changing core-well and shell-well widths, the following conditions are to be fulfilled. The electron and hole must be located in the same well: in the core-well for the ground states and in the shell-well for the excited states. Herein, the intensity of interband transitions would be large due to the large overlapping of wave functions of quasiparticles in respective states. At the same time, the possibility of excitation relaxation due to the intraband transitions would be small because of different locations of quasiparticles in ground and excited states.

The abovementioned conditions can be created for the nanostructure without the on-center impurity with geometrical parameters: $r_0 = 6$ nm, $\rho = 4$ nm, $\Delta > 2$ nm. Presence of the impurity in the core-well dramatically reduces the oscillator strength of $1s$–$1s$ interband transition.

In order to create the emitting sources based on the intraband transitions, it is necessary to reduce the probability of relaxation of excitations via the interband transitions. The dependence of oscillator strength of $1p$–$1p$ interband transition has sharp minimum at $r_0 = 7$ nm for the case without impurity (thin dash curve in Fig. 5b) but it coincides with the minimum of $1p$–$1s$ intraband transition (thick dash curve in Fig. 5e). The on-center impurity in QDQW shifts these minima to the opposite sides, so at $r_0 = 8 \div 9$ nm the large magnitudes of oscillator strengths of intraband transitions correspond to the minimal values of F_{1p-1p}. The behavior of oscillator strength of intraband transition F_{2p-1s} is opposite to F_{1p-1s}. The maximum of F_{2p-1s} corresponds to the minimum of F_{1p-1s}. This fact is observed for the different dependences of oscillator strengths both for QDQW with and without impurity.

4. Summary

The energies and distributions of probability densities for the electron and hole in ground and excited states are obtained using the exact solutions of the Schrödinger equation for GaAs/Al_xGa_{1-x}As/GaAs/Al_xGa_{1-x}As QDQW with and without on-center impurity. The oscillator strengths of intra- and interband transitions are calculated. The optimal geometrical parameters of the nanostructure are estimated for the possibility of simultaneous light emission based on $1s$–$1s$ and $1p$–$1p$ interband quantum transitions. It is shown that on-center impurity in the core demolishes the possibility to fabricate light sources with multicolor emission. The radiation in the infrared range of spectrum on the base of $1p$–$1s$ and $2p$–$1s$ intraband transitions is studied.

References

[1] S. Krishna, *J. Phys. D, Appl. Phys.* **38**, 2142 (2005).

[2] V.I. Klimov, Ch.J. Schwarz, D.W. McBranch, C.A. Leatherdale, M.G. Bawendi, *Phys. Rev. B* **60**, R2177 (1999).

[3] Y. Chan, J.S. Steckel, P.T. Snee, J.-M. Caruge, J.M. Hodgkiss, D.G. Nocera, M.G. Bawendi, *Appl. Phys. Lett.* **86**, 073102 (2005).

[4] A. Moazzam, S. Chattopadhyay, A. Nag, A. Kumar, S. Sapra, S. Chakraborty, D.D. Sarma, *Nanotechnology* **18**, 075401 (2007).

[5] X. Wang, X. Yan, W. Li, K. Sun, *Adv. Mater.* **24**, 2742 (2012).

[6] X. Yang, D. Zhao, K.S. Leck, S.T. Tan, Y.X. Tang, J. Zhao, H.V. Demir, X.W. Sun, *Adv. Mater.* **24**, 4180 (2012).

[7] M.A. Kastner, *Rev. Mod. Phys.* **64**, 849 (1992).

[8] T. Mano, T. Kuroda, S. Sanguinetti, T. Ochiai, T. Tateno, J. Kim, T. Noda, M. Kawabe, K. Sakoda, G. Kido, N. Koguchi, *J. Nanophotonics* **3**, 031605 (2009).

[9] M. Heigoldt, J. Arbiol, D. Spirkoska, J.M. Rebled, C.S. Conesa-Boj, G. Abstreiter, F. Peiro, J.R. Morantece, A. Fontcuberta íMorral, *J. Mater. Chem.* **19**, 840 (2009).

[10] O.M. Makhanets, V.I. Gutsul, N.R. Tsiupak, O.M. Voitsekhivska, *Condens. Matter Phys.* **15**, 33704, (2012).

[11] S. Nizamoglu, E. Mutlugun, T. Ozel, H.V. Demir, S. Sapra, N. Gaponik, A. Eychmuller, *Appl. Phys. Lett.* **92**, 113110 (2008).

[12] S. Nizamoglu, H.V. Demir, *Opt. Expr.* **16**, 3515 (2008).

[13] M. Şahin, S. Nizamoglu, O. Yerli, H. Demir *J. Appl. Phys.* **111**, 023713 (2012).

[14] R. Kostić, D. Stojanović, *Phys. Scr. T* **149**, 014055 (2012).

[15] P. Tyagi, P. Kambhampati, *J. Phys. Chem. C* **116**, 8154 (2012).

[16] D. Schooss, A. Mews, A. Eychmüller, H. Weller, *Phys. Rev. B* **49**, 17072 (1994).

[17] M. Tkach, V. Holovatsky, O. Voitsekhivska, M. Mikhalyova, *Phys. Status Solidi B* **203**, 373 (1997).

[18] A. Lorke, R. Luyken, A. Govorov, J. Kotthaus, J. Garcia, P. Petroff, *Phys. Rev. Lett.* **84**, 2223 (2000).

[19] J. Planelles, J. Climente, *Eur. Phys. J. B* **48**, 65 (2005).

[20] V. Holovatsky, O. Makhanets, O. Voitsekhivska, *Physica E* **41**, 1522 (2009).

[21] V.I. Boichuk, I.V. Bilynskyi, R.Ya. Leshko, *Condens. Matter Phys.* **13**, 13702 (2010).

[22] V.A. Holovatsky, I.B. Frankiv, *J. Optoelectron. Adv. Mater.* **15**, 88 (2013).

[23] H. Taş, M. Şahin, *J. Appl. Phys.* **112**, 053717 (2012).

[24] M. Sahin, K. Koksal, *Semicond. Sci. Technol.* **27**, 125011 (2012).

[25] I.F.I. Mikhail, S.B.A. El Sayed, *Physica E* **43**, 1371 (2011).